12th Int. Particle Acc. Conf. IPAC2021, Campinas, SP, Brazil JACoW Publishing
ISBN: 978-3-95450-214-1 ISSN: 2673-5490 doi:10.18429/JACoW-IPAC2021-THPAB229

ENERGY-BINNING FAST MULTIPOLE METHOD FOR ELECTRON INJECTOR SIMULATIONS

S. A. Schmid*, E. Gjonaj, H. De Gersem, TU Darmstadt, TEMF, Darmstadt, Germany

Abstract

We implemented an energy-binning (EB) scheme for a meshless fast multipole method (FMM). The approach approximates the momentum distribution of the electron beam by assigning particles to tree structures defined at different Lorentz frames. Based on the tree decomposition, the FMM computes a hierarchical approximation for the space charge interaction of the particle bunch. We apply the EB FMM to simulate the beam generation in the photoinjector of the European XFEL developed at DESY-PITZ. Furthermore, we present numerical convergence and performance studies and compare the simulation results to a Liénard-Wiechert (LW) model.

INTRODUCTION

The beam dynamics of a high brilliance electron source, such as the PITZ photoinjector of the European XFEL at DESY [1], is crucially influenced by space charge effects. Most common simulation codes rely on a computational grid to calculate an electroquasistatic (EQS) approximation of the space charge field in the co-moving Lorentz frame of the particles based on the average beam energy. The program IMPACT-T [2] additionally offers an extended interaction model based on the EB method [3]. The latter improves the field computation especially for charge distributions with a large energy spread such as particle beams in an electron injector. Our newly developed simulation code [4] calculates the space charge field with a meshless fast multipole method (FMM) [5]. This has the benefit that artificial grid effects like aliasing errors or unstable mode coupling do not occur. This contribution shows how the EB technique can be implemented in the FMM space charge computation.

ENERGY-BINNING FMM

Figure 1 shows the charge density of an electron bunch after beam generation in a photoinjector. The phase space distribution exhibits a comparably large energy spread of 30 % as well as a strong correlation $\rho\left(z,\gamma\right) = 1$ between the longitudinal position z and the relativistic Lorentz factor γ of the particles. Hence, an EQS approximation based on the mean particle energy $\langle\gamma\rangle \approx 1.2$ introduces significant errors for the space charge field as seen in Fig. 2 a) and 2 b).

The EB method [3] remedies for the effect of the energy spread by assigning the particles to N_b separate Lorentz frames. Then, the total space charge field corresponds to the superposition

$$\mathbf{E}\left(\mathbf{r}\right) = \sum_{b=1}^{N_b} \mathbf{E}_b\left(\mathbf{r}\right), \qquad \mathbf{B}\left(\mathbf{r}\right) = \sum_{b=1}^{N_b} \mathbf{B}_b\left(\mathbf{r}\right),$$

* schmid@temf.tu-darmstadt.de

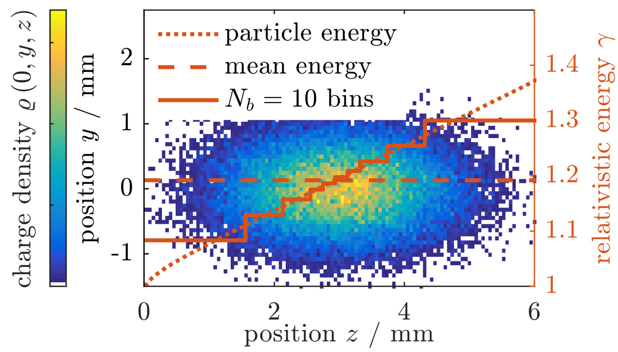

Figure 1: Particle distribution after beam generation.

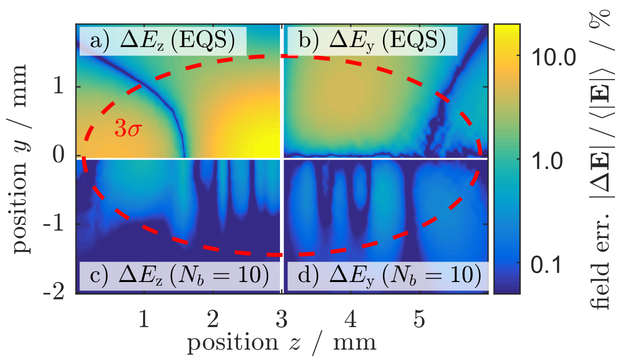

Figure 2: Space charge field error of the EQS model compared to an EB computation with $N_b = 10$ energy bins.

of the EQS approximations for the electric $\mathbf{E}_b$ and magnetic $\mathbf{B}_b$ fields in each individual Lorentz frame. Figure 1 shows the definition of $N_b = 10$ energy bins based on a recursive bisection method for the mean particle momentum. The EB model reduces the EQS error as shown in Fig. 2 c) and 2 d).

The conventional FMM [5] approximates far field contributions with multipole expansions and computes near field interactions as direct particle-particle evaluations based on a hierarchical tree structure. Our extension for the EB model uses a separate tree for each Lorentz frame $b = 1 \ldots N_b$. Figure 3 visualizes the tree structure corresponding to the bin $b = 1$ for the lowest energy $\gamma_1 = 1.08$ in Fig. 1. Besides the nodes that only contain source particles of the current energy bin $b = 1$ (blue triangles) there are also nodes that contain positions of particles from the other energy bins $b = 2 \ldots N_b$ (orange triangles) as well as mixed nodes (bicolored rhombi). The phase space correlation $\rho\left(z,\gamma\right) = 1$ of the particle distribution in Fig. 1 introduces a spatial separation between these three kinds of nodes.

The conventional refinement procedure of the FMM recursively subdivides the nodes of the tree structure until each child node represents less than $N_0 = const.$ particles.

ISBN: 978-3-95450-214-1 ISSN: 2673-5490 doi:10.18429/JACoW-IPAC2021-THPAB229

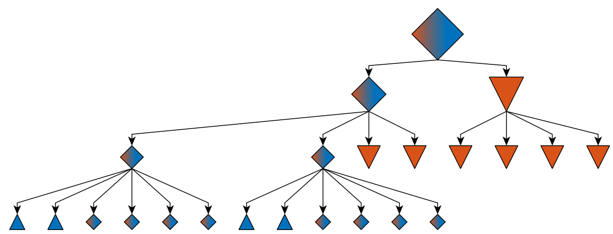

Figure 3: EB FMM tree for $b = 1$ out of $N_b = 10$. Triangles represent nodes solely containing source particles of $b = 1$ (blue) or particle positions from other bins (orange).

However, for the EB FMM the number of field evaluation positions from the other energy bins $b = 2 \ldots N_b$ can be much larger than the number of source particles in $b = 1$. Hence, the conventional node refinement does not necessarily provide a good numerical efficiency. Our implementation uses an adaptive refinement procedure to generate a tree structure which is more suitable for the EB model. First, an EB specific refinement criterion of $N_0' = N_0/\sqrt{N_b}$ limits the number of node internal particle-particle computations to ${N_0}^2$. Second, unnecessary refinement levels of nodes that require less than ${N_0}^2$ particle-particle interactions with their nearest neighbours are removed.

Figure 4 shows how the adaptive refinement procedure reduces the number of FMM operations for both the far field multipole to local (M2L) approximations and the near field particle to particle (P2P) interactions. For a particle beam without phase space correlation $\rho = 0$ the adaptive tree increases the numerical efficiency by balancing the M2L and the P2P operations. Spatial decoupling of the nodes in the tree structure of a particle beam with phase space correlation $\rho = 1$, such as for an electron injector, reduces the M2L operations significantly.

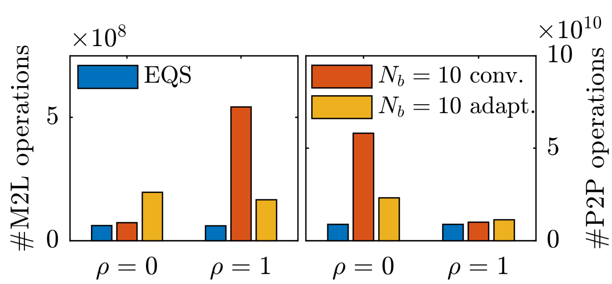

Figure 4: Number of FMM computer operations for far field approximation (M2L) and near field evaluation (P2P).

The runtime of the FMM space charge field computation in Fig. 5 a) depends linearly on the number of energy bins N_b and shows a slope that is smaller than one. Hence, each field evaluation at all N positions for the source particles contained in one energy bin requires less computational effort than approximating the space charge interaction of the full N particle ensemble. On the one hand, for $N_b \ll N$ the adaptive tree structure keeps the amount of near field evaluations P2P small enough such that the FMM approximation remains numerically efficient. On the other hand, some of the FMM far field evaluations at the particle positions from other energy bins do not require additional communications of multipole coefficients M2L thereby additionally reducing the computational effort. Aside from that, the spatial separation between the nodes for the leading and trailing particles in the beam with a correlated phase space $\rho = 1$ reduces the runtime of the FMM approximation even further.

Figure 5 b) shows the space charge field convergence as a function of N_b. For the particle beam with phase space correlation $\rho = 1$ even a small bin number $N_b \approx 4 - 8$ suppresses the field error induced by energy spread in EQS calculations sufficiently well. Due to spatial averaging of the field, the effect is less pronounced if the phase space is uncorrelated $\rho = 0$.

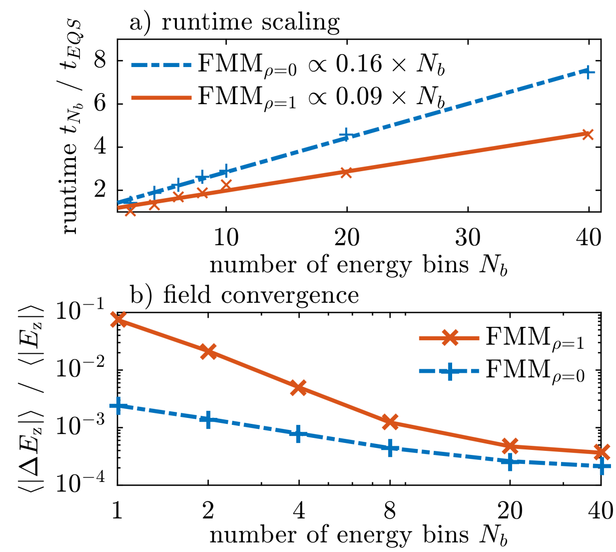

Figure 5: Runtime and convergence of the EB FMM with respect to the number of energy bins.

APPLICATION STUDIES

Figure 6 shows a numerical study for a space charge limited electron beam generation in a constant electric field of $E_z = 45\,\mathrm{MV/m}$. The simulation models a $Q_0 = 10\,\mathrm{nC}$ charge emission over a time span of $\Delta t = 0.22\,\mathrm{ns}$ from a circular spot with $d = 1.2\,\mathrm{mm}$ diameter out of a photocathode using $N = 10^7$ macroparticles. All macroparticles which propagate backwards through the cathode surface are removed from the simulation.

As a direct consequence of the EQS approximation, the cathode current of the simulation without EB in Fig. 6 a) artificially increases over time. Due to their spatial distance, the leading particles should not significantly influence the interactions at the photocathode surface. However, using the ensemble averaged Lorentz factor $\langle\gamma\rangle$ systematically underestimates the longitudinal space charge field of the trailing particles. In contrast, the cathode current of the simulation using $N_b = 5$ energy bins does not increase. After a transient start-up period the current saturates at a constant

ISBN: 978-3-95450-214-1 ISSN: 2673-5490 doi:10.18429/JACoW-IPAC2021-THPAB229

value for $t > 0.07$ ns. This behavior is expected once the space charge limitation reaches its steady state. The inset in Fig. 6 compares the relative portion R of macroparticles which were successfully emitted from the cathode. The EB model in Fig. 6 c) exhibits a homogeneous emission across the core region surrounded by a distinct ring. For the EQS model in Fig. 6 b) the relativistic dilation of the charge distribution blurs the transition between core and ring.

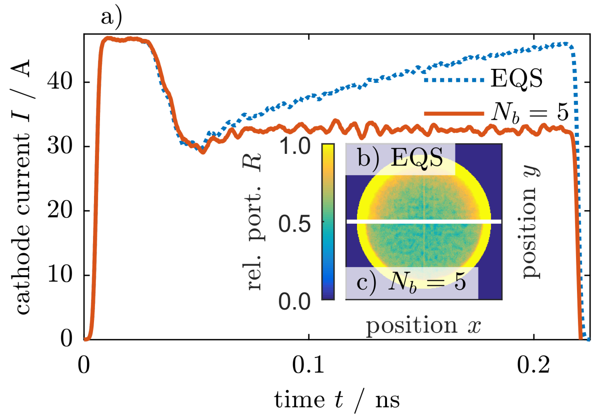

Figure 6: Space charge limited beam generation.

Figure 7 shows simulation results for a $Q = 1$ nC electron beam of the DESY-PITZ photoinjector [1] at a laser spot radius of $r = 0.8$ mm. The LW simulation uses a fully relativistic space charge model including both retardation and radiation effects based on each macroparticle's world line [6]. Such simulations are computationally extremely expensive and require a computing cluster. Furthermore, numerical efficiency restricts the macroparticle approximation to a rather small ensemble size of $N = 2.5 \cdot 10^5$.

A comparison of the transversal emittance ε_x in Fig. 7 a) demonstrates that the EB FMM with $N_b = 5$ includes additional effects caused by the energy spread of the beam. Especially the transversal slice emittance at the exit of the gun cavity in Fig. 7 b) shows a very good agreement with the LW simulation. In contrast, the field error of the EQS model results in a discrepancy. Unlike the LW model, the EB simulation benefits from the numerical efficiency of the hierarchical FMM approximation. Thus, the FMM approach can handle a significantly larger ensemble size $N \sim 10^7$ even on a workstation computer.

CONCLUSION

The meshless energy-binning fast multipole method provides a computationally efficient approach to compute space charge interactions in a particle beam with large energy spread. An adaptive refinement of the tree structures defined at different Lorentz frames reduces the number of computer operations. The approximation of the space charge field scales linearly with the number of energy bins with a proportionality constant smaller than one. Due to its numerical properties, the approach is particularly suitable for a particle

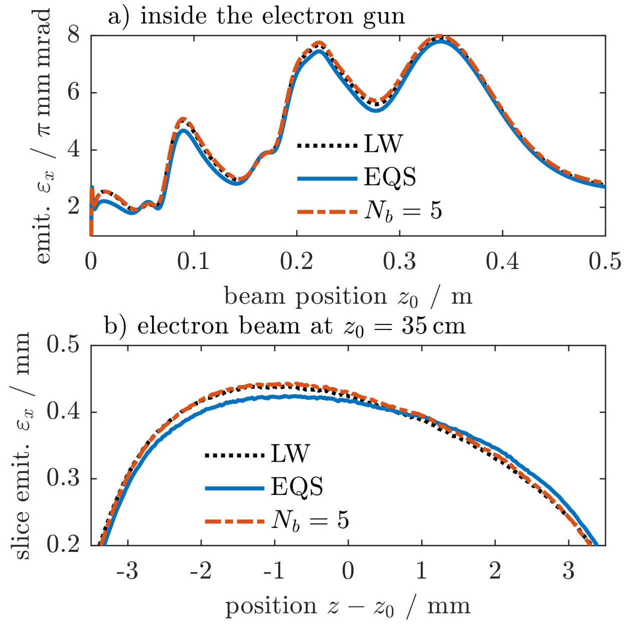

Figure 7: Simulation of the DESY-PITZ photoinjector.

distribution with correlated phase space such as the electron beam of a photoinjector. Two numerical studies demonstrate typical applications for the newly implemented simulation program. One major advantage of the hierarchical space charge approximation is that it facilitates simulations of large macroparticle ensembles without introducing artificial grid effects.

REFERENCES

[1] M. Krasilnikov *et al.*, "Experimentally minimized beam emittance from an L-band photoinjector", *PRSTAB*, vol. 15, p. 100701, Oct. 2012. doi:10.1103/PhysRevSTAB.15.100701

[2] J. Qiang, S. Lidia, R. D. Ryne, and C. Limborg-Deprey, "Three-dimensional quasistatic model for high brightness beam dynamics simulation", *PRSTAB*, vol. 9, p. 044204, Apr. 2006. doi:10.1103/PhysRevSTAB.9.044204

[3] G. Fubiani, J. Qiang, E. Esarey, W. P. Leemans, and G. Dugan, "Space charge modeling of dense electron beams with large energy spreads", *PRSTAB*, vol. 9, p. 064402, Jun. 2006. doi:10.1103/PhysRevSTAB.9.064402

[4] S. A. Schmid, E. Gjonaj, and H. De Gersem, "Simulating space charge dominated beam dynamics using FMM", in *Proc. NAPAC'19*, Lansing, MI, USA, Sept. 2019, paper WEPLE10, pp. 909-911.

[5] L. Greengard and V. Rokhlin, "A fast algorithm for particle simulations", *J. Comput. Phys.*, vol. 73, pp. 325-348, Feb. 1987. doi:10.1016/0021-9991(87)90140-9

[6] Y. Chen, M. Krasilnikov, F. Stephan, E. Gjonaj, T. Weiland, and M. Dohlus, "Modeling and simulation of RF photoinjectors for coherent light source", *NIMA*, vol. 889, pp. 129-137, May 2018. doi:10.1016/j.nima.2018.02.017